Dalton Transactions

C(sp3)-H Oxidation and Chlorination Catalysed by A Bioinspired Pincer Iron(III) Complex

Journal:	*Dalton Transactions*
Manuscript ID	DT-COM-06-2022-002005.R1
Article Type:	Communication
Date Submitted by the Author:	13-Jul-2022
Complete List of Authors:	Han, Jian; Utah State University, Chemistry and Biochemistry; Penn State University Park, chemistry Tan, Liming; Utah State University Wan, Yanjun; Utah State University, Chemistry and Biochemistry; Columbia University, Chemistry Li, Gang; Utah State University, Chemistry and Biochemistry Anderson, Stephen; Utah State University, Chemistry and Biochemistry

COMMUNICATION

C(sp³)-H Oxidation and Chlorination Catalysed by A Bioinspired Pincer Iron(III) Complex

Jian Han, Liming Tan, Yanjun Wan, Gang Li,* and Stephen N. Anderson

Received 00th January 20xx,
Accepted 00th January 20xx

DOI: 10.1039/x0xx00000x

A pincer iron(III) catalyst for the oxidation and chlorination of C(sp³)-H bonds was developed. Oxidation of a diagnostic substrate cis-decalin implies a long-lived carbon-centred radical is involved. Mechanistic studies suggest that a Fe-oxo species could be responsible for the rate-determining C-H activation step. This report expanded the scope of non-heme catalysts for C-H functionalisation.

Direct functionalisation of C(sp³)-H bonds is highly valuable in modern chemical and pharmaceutical industries as it enables conventional diversifications of inexpensive chemical feedstocks into versatile building blocks in an atom-economical manner.[1, 2] This transformation, however, remains a challenge due to the high bond dissociation energy (BDE) of C-H bond (90-100 kcal·mol^{-1}).[3] Nature has evolved an efficient way to functionalise the C(sp³)-H bond using a diverse range of enzymes with metal cofactors.[4, 5] A high valent metal oxo species is responsible for C-H activation by abstracting a hydrogen atom from the C-H bond.[6] Synthetic models have been extensively studied to mimic the reactivity of enzymes. To date, many efforts have been devoted to iron catalysts due to their high availability and high reactivity. While a variety of amine-based ligands has been used as models for *non-heme* enzymes,[7-12] only porphyrin ligands have been employed to mimic *heme* enzymes to date.[6, 8, 12-14] Metalloporphyrin catalysts (*heme* models) have demonstrated diverse reactivities in C-H functionalization.[6] However, the limited variations and synthetical difficultness of porphyrin ligands prohibit flexibility in ligand design, which further limits their practicality. In contrast, non-heme catalysts are more flexible in structures and easier to prepare, but they are usually vulnerable towards oxidative decomposition due to the oxidation of the weak C-H bonds on the ligand.[15, 16]

Department of Chemistry and Biochemistry, Utah State University, Logan, Utah, 84322, USA. E-mail: gang.li@usu.edu
Electronic Supplementary Information (ESI) available: [details of any supplementary information available should be included here]. See DOI: 10.1039/x0xx00000x

It is advantageous if a catalyst combines the benefits of both *heme* and *non-heme* systems. Recently, a tridentate iron catalyst bearing a carbazole pincer ligand has drawn our attention.[17] This carbazole pincer ligand possesses a planar structure along with a strong electron-donating ability, which is similar to a porphyrin ligand. Moreover, this catalyst can catalyse the epoxidation of olefins with heme-like selectivity, presumably via a concerted oxygen atom transfer process. This seminal work shed light on the feasibility to use non-heme pincer catalysts towards C-H functionalisation. Herein, we discuss the C-H oxidation of aliphatic and benzylic substrates by a non-heme pincer iron complex (Scheme 1). Using *m*-chloroperoxybenzoic acid (*m*CPBA) as the terminal oxidant, the catalytic system shows high oxidation reactivity towards unactivated C(sp³)-H bonds. More delightfully, if sodium hypochlorite (NaOCl) is added, the iron pincer complex can catalyse C-H chlorination, representing one of the rare examples of C-H halogenation by a non-heme iron complex.[18-25]

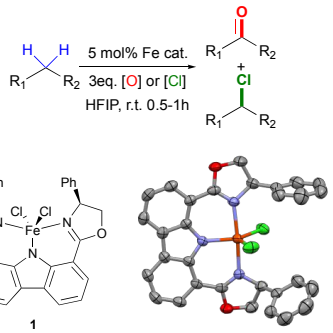

1

Scheme 1. C(sp³)-H functionalisation catalyzed by non-heme iron(III) pincer catalyst and the X-ray crystal structure of the iron catalyst **1** (50% ellipsoids. Hydrogen atoms have been omitted for clarity).

We commenced our study by exploring the oxidation of cyclooctane, which is used as the limiting reagent (Table 1). Reaction was best performed when 5% catalyst was used with 3 equiv. of *m*CPBA in hexafluoroisopropanol (HFIP) under room temperature (Table 1, entry 1). A simple inorganic salt, $FeCl_3$, was able to catalyse the reaction, albeit in much lower

conversion even after 24 h (Table 1, entry 2). Adding a free ligand along with $FeCl_3$ salt also showed low efficiency (Table 1, entry 3), presumably due to the rapid decomposition of the free ligand under oxidizing conditions.[15, 16] When common solvents for C-H functionalisation reactions were tested, for instance acetonitrile and ethyl acetate, only low conversion of substrate was observed (Table 1, entries 4 and 5). A possible rationale for the advantage of using HFIP over non-fluorinated solvents is that the strong hydrogen donor ability of HFIP decreases the nucleophilicity of the oxygenation product phenol which prevents product inhibition and allows for higher catalytic turnover numbers. Similar effect was recently observed in the aromatic C-H oxidation by a manganese catalyst.[26] Oxidant is another important character in the reaction. The H_2O_2/CH_3CO_2H oxidative system, which showed high efficiency in C-H oxidation reactions in other non-heme iron catalytic systems,[27-29] gave only minimal conversion (Table 1, entry 6). Iodosylbenzene (PhIO), a widely used oxo transfer reagent, lead to trace conversion due to fast ligand decomposition (Table 1, entry 7). Another peracid oxidant, peracetic acid (CH_3CO_3H), showed only moderate efficiency (Table 1, entry 8). The amount of oxidant was also investigated (Table 1, entries 9 and 10). A low oxidant loading gave low conversion while over-oxidation was observed under high oxidant loading. Slow addition of oxidant via syringe pump over 2 h did not improve the reaction efficiency (Table 1, entry 11). Temperature is also a vital factor in the reaction (Table 1, entries 12 and 13). Decreasing the temperature to 0 °C and extending reaction time to 12 h only gave low conversion while increasing the reaction temperature to 50 °C lead to fast overoxidation of desired product. Carrying out the reaction under inert atmosphere showed no significant influence (Table 1, entry 14).

Table 1. Optimization of oxidation reaction[a]

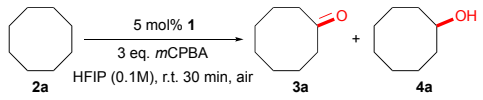

Entry	Deviation from standard condition	Conv. (%)	Yield (%)	
			3a	**4a**
1	none	74%	32%	25%
2	$FeCl_3$ instead of **1** for 24 h	23%	17%	5%
3	$FeCl_3$ + ligand instead of **1**	27%	18%	5%
4	CH_3CN instead of HFIP	20%	14%	<5%
5	Ethyl acetate instead of HFIP	19%	12%	<5%
6	H_2O_2/CH_3CO_2H instead of *m*CPBA	<5%	-	-
7	PhIO instead of *m*CPBA	<5%	-	-
8	CH_3CO_3H instead of *m*CPBA	25%	11%	11%
9	1 eq. *m*CPBA	33%	13%	14%
10	5eq. mCPBA	87%	37%	10%
11	Slow addition of *m*CPBA in 2 h	56%	33%	10%
12	0 °C instead of room temp.	15%	10%	3%
13	50 °C instead of room temp.	85%	25%	9%
14	Under N_2	68%	30%	21%

[a] Conversions and yields were determined by GC-MS using dodecane as an internal standard. Multi-oxygenated compounds were major side products.

Table 2. Substrate scope of C(sp^3)-H Oxidations[a]

Substrate	Product	A/K
2a[b] (74% conv.)	**3a**, 32%; **4a**, 25%	0.8
2b[b] (68% conv.)	**3b**, 10%; **4b**, 31%	3
2c[b] (62% conv.)	**3c**, 29%; **4c**, 15%	0.5
2d[b] (40% conv.)	**3d**, 21%; **4d**, 17%	0.8
2e (>95% conv.)	**4e**, 77%	/
2f (92% conv.)[c]	*cis*-**4f**, 42%; *trans*-**4f**, 39%	7
2g (59% conv.)	**3g**, 50%	/
2h: R = H (>95% conv.)[b] **2i**: R = OAc (>95% conv.) **2j**: R = Cl (>95% conv.) **2k**: R = CN (40% conv.) **2l**: R = NO_2 (51% conv.)	**3h**, <5% **3i**, 55% **3j**, 59% **3k**,32% **3l**, 42%	/
2m (>95% conv.)	**3m**, 78%	/
2n (>95% conv.)	**3n**, 47%	/

[a] Reaction condition: 0.5 mmol substrate, 5% catalyst, 1.5 mmol *m*CPBA, 5 mL HFIP at room temperature for 30 min. Isolated yields were reported if not specified. A/K is the alcohol-to-ketone ration, A = alcohols, K = ketones. [b] Yields were determined by GC-MS using dodecane as an internal standard. [c] Ketone products were also observed in 10% yield by GC-MS using dodecane as an internal standard, see Figure S5 in Supporting Information.

Under the optimized condition, we then investigated the scope for the C(sp^3)-H oxidation reaction (Table 2). Both aliphatic and benzylic substrates smoothly afforded the desired oxidation products with moderate to good yields. Cycloalkane substrates with only 2° C-H bond (**2a**-**2d**) afforded both ketone and alcohol products. Substrates with both accessible 2° C-H bonds and 3° C-H bonds (**2e** and **2f**) showed high tertiary selectivity. The desired alcohol products in good yields suggests a highly selective metal-oxo species is involved in the reaction.[30,

[31] Furthermore, activated C-H bonds were preferentially oxidized. In a terpenoid compound (-)-ambroxide (**2g**), only the activated methylenic 2° C-H bonds adjacent to oxygen was oxidized, providing the lactone product in 31% yield.

When benzylic substrates (**2h**-**2n**) were subjected to the reaction condition, only ketone derivatives were observed as the main products. Substrates with electron-rich substituents (**2h**) degraded quickly under catalytic condition, indicating a highly oxidizing reaction system. Substrates with electron-withdrawing substituents (**2i**-**2l**) were better tolerated and able to provide oxidation product with moderate yield, albeit in lower conversion. This oxidation process has also been applied to the functionalisation of bioactive molecules. Both celestolide (**2m**) and ibuprofen methyl ester (**2n**) were oxidized at the benzylic position with other functional groups intact.

It is important to note that in the oxidation of aliphatic substrates, ketones are observed in an appreciable amount. The alcohol-to-ketone ratio (A/K) observed for cyclooctane (**2a**) is approximately 1:1. It has been shown recently that HFIP deactivates alcohols towards further oxidations and enhance hydroxylation selectivity in Fe and Mn catalysed oxidation reactions.[32] Thus, the ketone products are unlikely formed due to over-oxidation of alcohol. Instead, the small A/K ratio in this work suggested the existence of a long-lived radical species that could undergo Russell termination.[33, 34] A more convincing evidence is the oxidation of *cis*-decalin (**2f**), where a mixture of *cis*-decalol (*cis*-**4f**) and *trans*-decalol (*trans*-**4f**) was observed in a ratio of 1:1. The large amount of radical rearranged product *trans*-decalol further supports that a long-lived radical intermediate is involved in the reaction[35, 36].

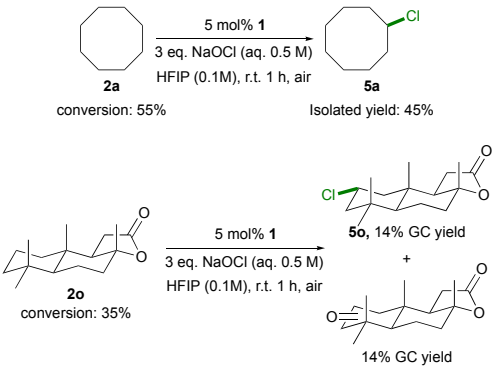

Scheme 2. (A). Chlorination of cyclooctane. (B) Chlorination of (+)-sclareolide.

This long-lived radical species could enable C-H functionalisation other than oxidation, including C-H halogenation reactions, similar to that in a manganese porphyrin system.[37] In fact, C-H halogenation catalysed by a biomimetic iron catalyst remains a challenge and very rare examples have been reported.[19, 25] Complexes capable of performing C-H halogenation typically involve the use of a stoichiometric amount of iron halide complexes to outpace the fast oxidation process[18-21, 23, 25, 38]. If *m*CPBA was replaced by sodium hypochlorite (NaOCl) in the oxidation condition, chlorination products were indeed observed (Scheme 2A) with only trace oxidation product. If no catalyst is added, only trace oxygenation product was observed and no chlorination product was detected, highlighting the necessity of the iron catalyst. It was noted that the catalyst decomposed faster under the chlorination condition due to high oxidizing ability of NaOCl, which resulted in lower substrate conversion than in oxidation reaction. However, the high oxidizing ability could also be beneficial. A plant-derived terpenoid, (+)-sclareolide, gave only trace conversion under the oxidation condition. Significantly, a C2 equatorial chloride was observed under the chlorination condition, along with equal amount of oxidation side products (Scheme 2B and Figure S6 in Supporting Information). Such reactivity was also observed in C-H chlorination reaction catalysed by a manganese porphyrin.[37]

To gain more insight into the mechanism of C-H activation, spectroscopic analyses were conducted on the iron catalyst to further elucidate its function in the reaction (Figure 1). At 0 °C, catalyst **1** exhibits absorbance at 320 nm and a weak signal at 630 nm in HFIP. Upon addition of *m*CPBA (1 equiv.), both signals at 320 nm and 630 nm quickly disappeared. Meanwhile, a new peak at 670 nm was observed. This peak at 670 nm is typically observed in iron porphyrin systems, which is assigned to an oxoiron(IV) π-cation radical species.[39, 40] Similar peaks were also observed by Niwa and Takada on an analogue iron pincer complex with PhIO, where the structure was confirmed as an oxoiron(IV) π-cation radical by EPR.[17]

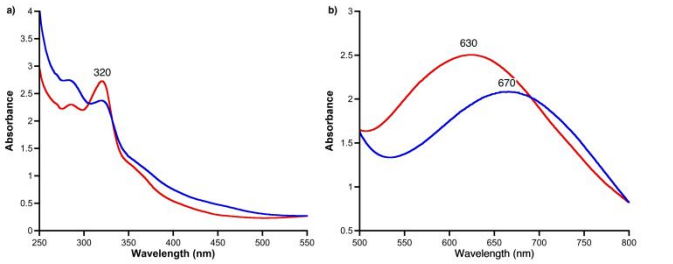

Figure 1. UV-vis spectra of catalyst **1** with *m*CPBA: a) [**1**] = 16 μM; b) [**1**] = 1.6 mM. Red line: **1** in HFIP at 0 °C; blue line: 10 s after the addition of *m*CPBA (1 equiv) at 0 °C.

The species at 670 nm also reacts with the substrate to regenerate the Fe(III) species. If a large excess of substrate was used, the reaction is pseudo-first order in the concentration of the iron oxo species (Figure 2).

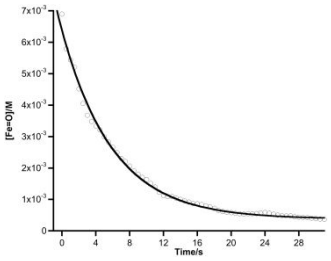

Figure 2. Decay of the *in situ* generated oxoiron species in the presence of cyclooctane at 0 °C. [Fe] = 0.8 mM, [mCPBA] = 0.8 mM, [cyclooctane] = 16 mM.

The rate law is thus described as:

$$-\frac{\mathrm{d[Fe=O]}}{\mathrm{d}t} = k[\mathrm{Fe=O}][\mathrm{cyclooctane}] = k_{\mathrm{obs}}[\mathrm{Fe}=\mathrm{O}]$$

the observed pseudo-first order rate constants k_{obs} are linearly dependent on the substrate concentration, which give a second-order rate constant k of 11.3(7) $M^{-1} s^{-1}$ (Figure 3, also see Figures S7-S11 in Supporting Information for details).

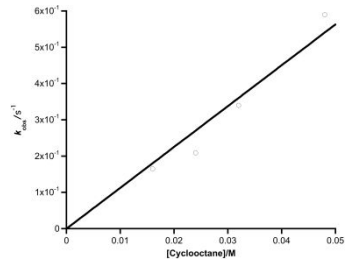

Figure 3. Observed pseudo-first order rate constant k_{obs} vs [cyclooctane]. All k_{obs} measured at 0 °C.

Furthermore, we studied the kinetic isotopic effect (KIE) of this oxidation reaction by conducting intermolecular competition experiments with cyclohexane (**2b**) and deuterated cyclohexane (**2b**-d_{12}) at room temperature (Scheme 3). The value of KIE (k_H/k_D) was 3.8, which suggests that C-H abstraction is rate-determining. This value is in agreement with those measured from C(sp^3)-H oxidation reactions catalysed by metal-based oxidant (KIE = 3-5),[41,42] including metal-oxo species.[6, 43]

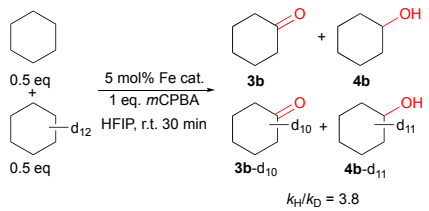

Scheme 3. Kinetic isotope effect study using cyclohexane and cyclohexane-d_{12}. k_H/k_D = ([**3b**]+[**4b**])/([**3b**-d_{10}]+[**4b**-d_{11}]).[**3b**-d_{10}] and [**4b**-d_{11}] calculated with the response factor of **3b** and **4b** respectively.

A possible mechanism is proposed based on above studies (Figure 4). In the presence of oxidant, an iron oxo complex will abstract a hydrogen atom from C-H bonds, resulting the formation of an alkyl or benzylic radical. This radical will subsequently rebound to the oxygen or chlorine atom to yield the desired oxidation or chlorination product.

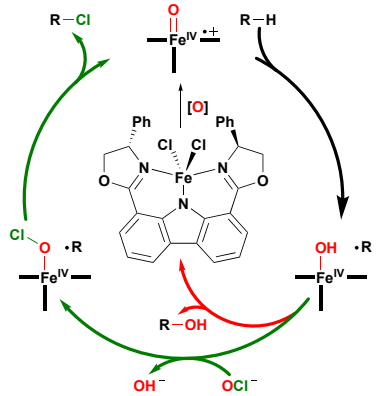

Figure 4. Proposed mechanism for the Fe catalyzed C(sp^3)-H functionalisation. Red pathway: oxidation. Green pathway: chlorination.

Conclusions

In closing, we have reported the use of a non-heme iron complex bearing a carbazole-based pincer ligand to effectively catalyze the oxidation of C(sp^3)-H bonds under mild condition. The rate-determining step is confirmed to be the H-abstraction by an iron-oxo intermediate. A long-lived radical intermediate was generated during the reaction. This radical can also enable the C-H chlorination by simply adding a chlorine source. Such reactivity for a non-heme iron catalyst is rare and we anticipate this catalytic system could be widely applied in late-stage functionalisation of bioactive molecules.

Conflicts of interest

There are no conflicts to declare.

Accession Codes

CCDC 2086380 contains the supplementary crystallographic data for this paper. This data can be obtained free of charge via www.ccdc.cam.ac.uk/data_request/cif, or by emailing data_request@ccdc.cam.ac.uk, or by contacting The Cambridge Crystallographic Data Centre, 12 Union Road, Cambridge CB2 1EZ, UK; fax: +44 1223 336033.

Acknowledgements

The authors thank the National Science Foundation (CHE-1429195 for Brüker Avance III HD 500 MHz NMR; CHE-1828764 for Rigaku Benchtop XtaLAB Mini II X-ray diffractometer). G.L. thanks Utah State University for the start-up fund.

References

1. T. Newhouse and P. S. Baran, *Angew. Chem. Int. Ed.*, 2011, **50**, 3362-3374.
2. L. McMurray, F. O'Hara and M. J. Gaunt, *Chem. Soc. Rev.*, 2011, **40**, 1885-1898.
3. Y.-R. Luo, *Comprehensive Handbook of Chemical Bond Energies*, CRC Press, Boca Raton, 2007.
4. D. Ringe and G. A. Petsko, *Science*, 2008, **320**, 1428.
5. S. P. d. Visser and D. Kumar, eds., *Iron-Containing Enzymes: Versatile Catalysts of Hydroxylation Reactions in Nature*, RSC Publishing, Cambridge, UK, 2011.
6. X. Huang and J. T. Groves, *Chem. Rev.*, 2018, **118**, 2491-2553.
7. M. Costas, M. P. Mehn, M. P. Jensen and L. Que, *Chem. Rev.*, 2004, **104**, 939-986.
8. W. Nam, *Acc. Chem. Res.*, 2007, **40**, 522-531.
9. L. Que, *Acc. Chem. Res.*, 2007, **40**, 493-500.
10. W. N. Oloo and L. Que, *Acc. Chem. Res.*, 2015, **48**, 2612-2621.
11. O. Y. Lyakin, K. P. Bryliakov and E. P. Talsi, *Coord. Chem. Rev.*, 2019, **384**, 126-139.
12. A. C. Lindhorst, S. Haslinger and F. E. Kühn, *Chem. Commun.*, 2015, **51**, 17193-17212.

13. B. Meunier, *Chem. Rev.*, 1992, **92**, 1411-1456.
14. X. Huang and J. T. Groves, *J. Biol. Inorg. Chem.*, 2017, **22**, 185-207.
15. K. Nehru, M. S. Seo, J. Kim and W. Nam, *Inorg. Chem.*, 2007, **46**, 293-298.
16. M. Grau, A. Kyriacou, F. Cabedo Martinez, I. M. de Wispelaere, A. J. P. White and G. J. P. Britovsek, *Dalton Trans.*, 2014, **43**, 17108-17119.
17. T. Niwa and M. Nakada, *J. Am. Chem. Soc.*, 2012, **134**, 13538-13541.
18. T. Kojima, R. A. Leising, S. Yan and L. Que, *J. Am. Chem. Soc.*, 1993, **115**, 11328-11335.
19. P. Comba and S. Wunderlich, *Chem. Eur. J.*, 2010, **16**, 7293-7299.
20. O. Planas, M. Clémancey, J.-M. Latour, A. Company and M. Costas, *Chem. Commun.*, 2014, **50**, 10887-10890.
21. M. Puri, A. N. Biswas, R. Fan, Y. Guo and L. Que, *J. Am. Chem. Soc.*, 2016, **138**, 2484-2487.
22. N. Kannan, A. R. Patil and A. Sinha, *Dalton Trans.*, 2020, **49**, 14344-14360.
23. S. Rana, J. P. Biswas, A. Sen, M. Clémancey, G. Blondin, J.-M. Latour, G. Rajaraman and D. Maiti, *Chem. Sci.*, 2018, **9**, 7843-7858.
24. J. P. Biswas, S. Guin and D. Maiti, *Coord. Chem. Rev.*, 2020, **408**, 213174.
25. K. Bleher, P. Comba, D. Faltermeier, A. Gupta, M. Kerscher, S. Krieg, B. Martin, G. Velmurugan and S. Yang, *Chem. Eur. J.*, 2022, **28**, e202103452.
26. E. Masferrer-Rius, M. Borrell, M. Lutz, M. Costas and R. J. M. Klein Gebbink, *Adv. Synth. Catal.*, 2021, **363**, 3783-3795.
27. M. S. Chen and M. C. White, *Science*, 2007, **318**, 783.
28. M. S. Chen and M. C. White, *Science*, 2010, **327**, 566.
29. P. E. Gormisky and M. C. White, *J. Am. Chem. Soc.*, 2013, **135**, 14052-14055.
30. A. Company, I. Prat, J. R. Frisch, D. R. Mas-Ballesté, M. Güell, G. Juhász, X. Ribas, D. E. Münck, J. M. Luis, L. Que Jr and M. Costas, *Chem. Eur. J.*, 2011, **17**, 1622-1634.
31. P. Comba, S. Fukuzumi, H. Kotani and S. Wunderlich, *Angew. Chem. Int. Ed.*, 2010, **49**, 2622-2625.
32. V. Dantignana, M. Milan, O. Cussó, A. Company, M. Bietti and M. Costas, *ACS Cent. Sci.*, 2017, **3**, 1350-1358.
33. G. A. Russell, *J. Am. Chem. Soc.*, 1957, **79**, 3871-3877.
34. J. Kim, R. G. Harrison, C. Kim and L. Que, *J. Am. Chem. Soc.*, 1996, **118**, 4373-4379.
35. J. T. Groves, W. J. Kruper and R. C. Haushalter, *J. Am. Chem. Soc.*, 1980, **102**, 6375-6377.
36. W. Liu, M.-J. Cheng, R. J. Nielsen, W. A. Goddard and J. T. Groves, *ACS Catal.*, 2017, **7**, 4182-4188.
37. W. Liu and J. T. Groves, *J. Am. Chem. Soc.*, 2010, **132**, 12847-12849.
38. S. Chatterjee and T. K. Paine, *Angew. Chem. Int. Ed.*, 2016, **55**, 7717-7722.
39. J. T. Groves and Y. Watanabe, *J. Am. Chem. Soc.*, 1986, **108**, 507-508.
40. S. R. Bell and J. T. Groves, *J. Am. Chem. Soc.*, 2009, **131**, 9640-9641.
41. G. Olivo, O. Lanzalunga and S. Di Stefano, *Adv. Synth. Catal.*, 2016, **358**, 843-863.
42. C-H abstraction by a peroxyl radical also has a KIE value in that range. See reference 30 for example.
43. A. Sorokin, A. Robert and B. Meunier, *J. Am. Chem. Soc.*, 1993, **115**, 7293-7299.